PCCP

Accepted Manuscript

This article can be cited before page numbers have been issued, to do this please use: J. Algaba, J. M. Míguez, B. Mendiboure and F. J. Blas, *Phys. Chem. Chem. Phys.*, 2019, DOI: 10.1039/C9CP01597C.

This is an Accepted Manuscript, which has been through the Royal Society of Chemistry peer review process and has been accepted for publication.

Accepted Manuscripts are published online shortly after acceptance, before technical editing, formatting and proof reading. Using this free service, authors can make their results available to the community, in citable form, before we publish the edited article. We will replace this Accepted Manuscript with the edited and formatted Advance Article as soon as it is available.

You can find more information about Accepted Manuscripts in the author guidelines.

Please note that technical editing may introduce minor changes to the text and/or graphics, which may alter content. The journal's standard Terms & Conditions and the ethical guidelines, outlined in our author and reviewer resource centre, still apply. In no event shall the Royal Society of Chemistry be held responsible for any errors or omissions in this Accepted Manuscript or any consequences arising from the use of any information it contains.

ROYAL SOCIETY OF CHEMISTRY

rsc.li/pccp

View Article Online
DOI: 10.1039/C9CP01597C

Journal Name

ARTICLE TYPE

Cite this: DOI: 00.0000/xxxxxxxxxx

An accurate density functional theory for the vapor-liquid interface of chain molecules based on the statistical associating fluid theory for potentials of variable range for Mie chainlike fluids

Jesús Algaba,[a] José Manuel Míguez,[a] Bruno Mendiboure[b] and Felipe J. Blas,*[a]

Received Date
Accepted Date

DOI: 00.0000/xxxxxxxxxx

A new Helmholtz free energy density functional is presented to predict the vapor-liquid interface of chainlike molecules. The functional is based on the last version of the statistical associating fluid theory for potentials of variable range for homogeneous Mie chainlike fluids (SAFT-VR Mie). Following the standard formalism, the density functional theory (SAFT-VR Mie DFT) is constructed using a perturbative approach in which the free energy density contains a reference term to describe all the short-range interactions treated at the local level, and a perturbative contribution to account for the attractive perturbation which incorporates the long-range dispersive interactions. In this first work, we use a mean-field version of the theory in which the pair correlations are neglected in the attractive term. The SAFT-VR Mie DFT formalism is used to examine the effect of molecular chain length and the repulsive exponent of the intermolecular potential on density profiles and surface tension of linear chains made up to six Mie (λ_r-6) segments with different values of the repulsive exponent of the intermolecular potential. Theoretical predictions from the theory are compared directly with molecular simulation data for density profiles and surface tension of Mie chainlike molecules taken from the literature. Agreement between theory and simulation data is good for short-chain molecules at all thermodynamic conditions of coexistence considered. Once the theory has proven that is able to predict the interfacial properties, and particularly interfacial tension, the SAFT-VR Mie DFT formalism is used to predict the interfacial behavior of two new coarse-grained models for carbon dioxide and water recently proposed in the literature. In particular, the theoretical formalism, in combination with the coarse-grained models for carbon dioxide and water, is able to predict the interfacial properties of these important substances in a reasonable way.

1 Introduction

Interfacial phenomena of complex substances and their mixtures play a central role in broad areas of applied science and industrial engineering processes, apart from the inherent interest on the fundamental nature of interfaces. Formation of micelles by amphiphilic surfactant molecules in aqueous solutions, colloids in emulsions, exploration of oil resources or heterogeneous catalysts are just a few examples of systems in which an accurate knowledge of the most important interfacial properties, including surface tension and interfacial profiles, are key to an efficient and optimal design of industrial processes. However, although the modeling of interfacial systems remains a challenge due to their inhomogeneous nature, important advances in Statistical Mechanics theories and computer simulation techniques, as well as the rapid development of computer hardware, have produced a large body of literature devoted to the description and estimation of interfacial properties of pure fluids and their mixtures.

From a methodological point of view, interfacial properties of complex fluids can be investigated from experiments, theoretical formalisms, and computer simulation techniques. Apart from experiments, which allow to determine some of the most relevant interfacial properties of a given system, molecular modeling, i.e., a collection of microscopic models and tools based on a molecular perspective of the system, has been focused on understanding

[a] Laboratorio de Simulación Molecular y Química Computacional, CIQSO-Centro de Investigación en Química Sostenible and Departamento de Ciencias Integradas, Universidad de Huelva, 21007 Huelva, Spain.
[b] Laboratoire des Fluides Complexes et Leurs Réservoirs, UMR5150, Université de Pau et des Pays de l'Adour, B. P. 1155, Pau Cdex 64014, France.
* Corresponding author, e-mail: felipe@uhu.es

View Article Online
DOI: 10.1039/C9CP01597C

the inhomogeneous fluid behavior of a great number of model and real systems of industrial interest. It is obvious that a quantitative evaluation and comprehension of the interfacial properties of complex systems can be only developed by starting from an accurate representation of the bulk homogeneous fluids.

Over last decades, molecular modeling has been also developed to gain an in deep understanding of bulk homogeneous fluid behavior. Among several possibilities, one of the most successful formalisms for the prediction of thermodynamic properties, and particularly fluid-phase equilibria, is the statistical associating fluid theory (SAFT) [1,2]. The general form of the SAFT expression of the Helmholtz free energy is based on the first-order perturbation theory (TPT1) for associating systems by Wertheim [3–6]. The total free energy comprises different contributions that take into account the total free energy of the systems from a rigorous Statistical Mechanics point of view. There exist a number of variants of this molecular-based equation of state (EOS) that have been developed over the last thirty-five years. The most relevant and used versions are: SAFT for variable range interaction (SAFT-VR) [7,8]; SAFT for Lennard-Jones (LJ) based segments (soft-SAFT) [9,10]; perturbed-chain SAFT based on the structure of the hard-sphere chain (PC-SAFT) [11]; cubic plus association (CPA) approach, in which the Wertheim theory of association in coupled with a cubic EOS, that extends the applicability of traditional cubic EOS to associating fluids [12]; and the SAFT-VR Mie 2006 EOS, proposed by Lafitte *et al.* [13], for model chain molecules formed from Mie segments interacting via $\lambda_r - \lambda_a$ Mie potential (with λ_r and $\lambda_a = 6$ the repulsive and attractive exponents). More recently, Lafitte *et al.* [14] proposed a new, specific and highly accurate version of SAFT for chain molecules formed from spherical segments that interact through Mie potential (SAFT-VR Mie EOS). The resulting theory is able to provide a high accuracy in the near-critical region, as well as an accurate description of second-derivative properties for chain molecules. This allows to represent globally the thermodynamic properties and fluid-phase equilibria of pure fluids and their mixtures with high precision. See the original work of Lafitte *et al.* [14] and the Supplementary Information for further details.

Although the different versions of SAFT that exit in the literature have been used to predict directly the thermodynamic and phase equilibria behavior of real substances from the knowledge of selected macroscopic experimental data for the vapor-liquid equilibria (liquid density and vapor pressure), other groups have used the information provided by this theoretical formalism to develop coarse grained (CG) models. CG methodologies aim to bridge the gap between the atomistic modeling of matter and the commonplace continuum description of fluids and solids. This can be done in a "*simple*" way by removing some of the (microscopic) degrees of freedom in the system to simplify its description, while at the same time attempting to maintain the thermodynamic description. Based on the success of the SAFT-VR Mie formalism, Jackson and co-workers have developed a new family of CG models for real substances known as SAFT-γ CG force fields [15–18]. This coarse-graining strategy is based on the assumption that real substances can be modeled as chain molecules formed from fused Mie segments. Under this perspective, and due to the high accuracy of the SAFT-VR Mie EOS predicting the behavior of real fluids and their mixtures, the theory is applied to obtain coarse-grained intermolecular potentials that can be used in molecular simulation over a wide range of thermodynamic conditions [17–21].

The development of the understanding of bulk homogeneous fluids behavior, in part due to the establishment of the Wertheim's ideas [19–21] and the different versions of the applied view of the theory, i.e., the SAFT formalism [17,18], as well as advances in computer simulation has allowed molecular modeling to provide a basis over which to develop and propose new theoretical formalisms and theories to deal with the most important interfacial properties of inhomogeneous fluids. One of the most interesting features of Wertheim's theory and particularly the SAFT EOS, is that can be used in combination with well-established methodologies for determining interfacial properties. This can be done effectively using statistical mechanics perturbative methods, such as the Density Gradient Theory (DGT) [22–26] and Density Functional Theory (DFT) [27–31].

One of the most sophisticated and successful theoretical treatments for the study of interfacial phenomena is undeniably DFT [27–31]. Contrary to DGT, the DFT formalism offers a complete predictive approach with no adjustable parameters. In general, the free-energy functional is divided in two parts: a reference term that incorporates only the ideal and short-range interactions, and a perturbative term in which the long-range interactions are taken into account. The reference term can be treated by using the LDA or with a weighted-density approximation (WDA). With the LDA, the energy contribution at a given point in the interface is approximated as that of the homogeneous fluid evaluated at the appropriate local density. By contrast, when using the WDA one proposes a weighted (smoothed) density over different points, which is a non-local functional of the original density, that depends on a number of weighting factors. Several authors have proposed different functions that define the density weights, the most common now being based on the fundamental measure theory (FMT) [32] and its variations (MFMT) [33,34]. The WDA has demonstrated to accurately reproduce the highly oscillatory profiles in confined systems near a wall [35–39], while the LDA approach provides a good representation of free fluid interfaces [40–44]. Comparisons of the performance and relative merits of the LDA and WDA methodologies can be found in the literature [45–47]. The fundamental details of the DFT approach can be found in the reviews on theoretical developments as well as on applications by Evans [28], Davis [27], Löwen [29], Wu [30,31], and Emborsky *et al.* [48]

There exist a significant number of theoretical approaches that exploit the accuracy of the Wertheim's theory or its applied version, the SAFT EOS, to describe the thermodynamic and structural behavior of inhomogeneous fluids: the Interfacial Statistical Associating Fluid Theory (iSAFT) originally proposed by Chapman and coworkers *et al.* [36,38,49–57], DFTs for polyatomic molecules, based on Wertheim TPT1, proposed by Kierlik and Rosinberg [58–60] and Yu and Wu [34,35] and used by other authors [61–66], and the versions of Gross and coworkers [67–71].

Finally, Blas *et al.* [41] and Gloor *et al.* [42] proposed a Helmholtz free energy density functional (SAFT-HS DFT) based on the sim-

View Article Online
DOI: 10.1039/C9CP01597C

plest SAFT EOS, the SAFT-HS[72–74], to predict the vapor-liquid interfacial properties of inhomogeneous fluids. In this equation, the bulk fluid is represented as a hard-core reference, the association is treated with Wertheim's first order perturbation theory[3–6], and a van der Waals mean-field approximation is used for the dispersive attractive interactions. This basic and simplified DFT formalism is able to provide a qualitative description of the most relevant interfacial properties of chainlike associating fluids as well as a quantitative comparison with experimental surface tension for selected systems including water and replacement refrigerants[41,42]. Several years ago, Gloor *et al.*[43] proposed a new DFT formalism based on the SAFT-VR approach to improve the description of the limiting behavior of the density profile away from the interface and to incorporate the correlations between molecules in the attractive term following a previous work of Toxvaerd[75]. The theory, and its extension proposed by Llovell *et al.*[40] for mixtures, is able to provide a good description of the interfacial properties of an important number of chainlike associating molecules[43] and experimental systems, including alkanes, alcohols, replacement refrigerants, water[44], and mixtures of relevance to reservoir engineering and reactive mixtures of carbon dioxide, water, and n-alkylamine in the context of carbon capture[76,77].

As it has been mentioned previously, Jackson, Galindo, Müller, Adjiman, and coworkers have proposed the new and extremely accurate SAFT formalism, the SAFT-VR Mie EOS[14], based on a reference monomer system characterized by a Mie potential of variable repulsive and attractive range. Using this new formalism, they have also developed a series of coarse-grained models generated using experimental data and the new EOS. The resulting formalism, which allows to obtain very accurate coarse-grained models for the simulation of molecular fluids, is known as SAFT-γ CG Mie force fields[17]. This approach, usually denoted by their authors as top-down technique, is based on the use of the accurate SAFT-VR Mie EOS to link the macroscopic properties of a fluid and the force-field parameters of the model. The combination of these two techniques allows one to obtain simple but highly accurate coarse-grained force fields for a great variety of complex molecules[17–21].

Under this perspective, we propose to combine the powerful DFT treatment for describing interfacial properties of complex systems with the highly accurate Helmholtz free energy of the SAFT-VR Mie formalism. In particular, the goal of this work is twofold: (1) to propose a new Helmholtz free energy density functional to describe fluid-fluid interfaces of chainlike molecules. The functional is based on the last version of the statistical associating fluid theory for potential of variable range of molecules formed from Mie segments (SAFT-VR Mie). This represents the natural extension of the SAFT-VR DFT formalism proposed by Gloor *et al.*[43] several years ago. To check if the theory is able to provide a good description of the most important interfacial properties, theoretical predictions are compared with recent results for Mie chainlike molecules made up to six Mie segments with different repulsive exponents[78]; (2) to use the novel coarse-grained SAFT-γ CG force fields based on the Mie potential for some compounds to check if the DFT formalism is able to describe accurately the most important vapor-liquid interfacial properties, with special emphasis on density profiles and interfacial tension. In particular, we asses the adequacy of the theory by comparing the interfacial properties obtained from the SAFT-VR Mie DFT with computer simulation results for the CG models of carbon dioxide and water proposed recently by Avendaño *et al.*[17] and Lobanova *et al.*[20], respectively. In addition to that, we also compare predictions from the proposed theory with experimental data taken from the literature.

The rest of the is organized as follows. In Section 2 we present the theory. Results and discussion, including simulation details, are presented in Section 3. Finally, in Section 4 we present the main conclusions.

2 Theory

In this work we consider chains of m_s tangent spherical segments of diameter σ which can interact through pair-wise interactions. The Mie potential is used to describe the monomer-monomer repulsive and dispersive interactions between the segments making up the molecules. This potential can be expressed as[79–82]

$$\phi(r) = \mathscr{C}\varepsilon\left[\left(\frac{\sigma}{r}\right)^{\lambda_r} - \left(\frac{\sigma}{r}\right)^{\lambda_a}\right] \tag{1}$$

with

$$\mathscr{C} = \left(\frac{\lambda_r}{\lambda_a}\right)^{\frac{\lambda_a}{\lambda_r-\lambda_a}} \tag{2}$$

where r denotes the distance between the centers of the two spherical segments, ε is the potential depth, and λ_a and λ_r are the attractive and repulsive exponents, respectively; the pre-factor $\mathscr{C}$ ensures that the minimum of the potential is at $-\varepsilon$ regardless of the values of exponents.

The Helmholtz free energy functional to deal with inhomogeneous fluids is based on the SAFT-VR Mie formalism proposed by Lafitte *et al.*[14] Details of this approach are provided in the Supplementary Information section.

We consider an open system at temperature T and chemical potential μ in a volume V. In the absence of external fields, the grand potential functional $\Omega[\rho(\mathbf{r})]$ of an inhomogeneous system is given by[28]

$$\Omega[\rho(\mathbf{r})] = A[\rho(\mathbf{r})] - \mu\int \mathrm{d}\mathbf{r}\,\rho(\mathbf{r}), \tag{3}$$

where $A[\rho(\mathbf{r})]$ is the intrinsic Helmholtz free energy functional. The minimum value of $\Omega[\rho(\mathbf{r})]$ is the equilibrium grand potential of the system and the corresponding equilibrium density profile $\rho_{\mathrm{eq}}(\mathbf{r})$ satisfies the following condition[28]:

$$\left.\frac{\delta\Omega[\rho(\mathbf{r})]}{\delta\rho(\mathbf{r})}\right|_{\mathrm{eq}} = \left.\frac{\delta A[\rho(\mathbf{r})]}{\delta\rho(\mathbf{r})}\right|_{\mathrm{eq}} - \mu = 0. \tag{4}$$

Following a standard perturbative approach[28,45] the intermolecular potential is partitioned into a reference term (which includes the ideal, hard-sphere, the perturbative due to the attractive interactions, and the chain contributions), and a perturbation attractive term (which includes the dispersive interactions

View Article Online
DOI: 10.1039/C9CP01597C

between the monomeric segments). In this work we consider the simplest level of approximation to account for the description of the vapor-liquid interface: the bulk fluid is treated at the SAFT-VR Mie level (a third-order perturbation theory which incorporates the correlations of the hard-sphere reference system), while the interfacial properties are treated at the mean-field level (the correlations are neglected in the dispersive term). This corresponds to the SAFT-VR Mie MF DFT according to the nomenclature proposed by Gloor *et al.*[43]. Following this work, we express the new Helmholtz free energy functional in terms of an ideal, a reference, and an attractive contribution,

$$A^{SAFT-VR}_{Mie,MF}[\rho(\mathbf{r})] = A^{IDEAL}[\rho(\mathbf{r})] + A^{REF}_{Mie,MF}[\rho(\mathbf{r})] + A^{ATT}_{Mie,MF}[\rho(\mathbf{r})]. \quad (5)$$

It is convenient to examine the gran potential functional in terms of the reduced free energy densities $f[\rho(\mathbf{r})] \equiv A[\rho(\mathbf{r})]/(Vk_BT) \equiv \rho(\mathbf{r})a[\rho(\mathbf{r})]$, where $a[\rho(\mathbf{r})] \equiv A[\rho(\mathbf{r})]/(Nk_BT)$.

As in the work of Gloor *et al.*[43], the reference term $A^{REF}_{\mathrm{Mie,MF}}[\rho(\mathbf{r})]$ incorporates all of the contributions to the free energy due to "short-range" interactions: the repulsive hard-sphere, the perturbative terms due to the attractive interactions, and the chain term,

$$A^{REF}_{Mie,MF}[\rho(\mathbf{r})] = A^{HS}[\rho(\mathbf{r})] + A^{SR}_1[\rho(\mathbf{r})] + A_2[\rho(\mathbf{r})] + A_3[\rho(\mathbf{r})] + A^{CHAIN}[\rho(\mathbf{r})] \quad (6)$$

Particular expression for the different contribution are included in the Supplementary Information section.

Following the work of Gloor *et al.*[43], the attractive term in the perturbative DFT treatment of an inhomogeneous fluid of chain-like molecules is described at the level of the van der Waals mean-field approximation in which the correlations due to attractive interactions are neglected. By making this approximation, the dispersive term can be written in the familiar mean-field form as

$$A^{\mathrm{ATT}}_{\mathrm{Mie,MF}}[\rho(\mathbf{r})] = \frac{1}{2}\int \mathrm{d}\mathbf{r}\, m_s\, \rho(\mathbf{r}) \int \mathrm{d}\mathbf{r}'\, m_s \rho(\mathbf{r}')\, \phi(|\mathbf{r}-\mathbf{r}'|). \quad (7)$$

Note that this is the form of the attractive free energy functional used in the SAFT-VR MF DFT formalism[43]. It is also important to recall here that the free energy given by Eq. (5) reduces to the bulk SAFT-VR Mie expression for a homogeneous system at constant density $\rho(\mathbf{r}) = \rho_{\mathrm{bulk}}$ (see Supplementary Information for further details).

The equilibrium density profile is the profile for which the Euler-Lagrange condition, i.e. Eq. (4), holds at every point $\mathbf{r}$. In this study we examine a planar vapor-liquid interface where the density is a function of the position normal to the interface. Assuming that the interface is perpendicular to the z-axis, the density profile depends only on the distance to the interface, i.e. $\rho(\mathbf{r}) \equiv \rho(z)$. The Euler-Lagrange equation is under-specified as any translation of the equilibrium density profile in the z direction is also a solution of Eq. (4). A unique solution is assured by specifying that $z_{\max}$ and $z_{\min}$ be the boundary values equivalent to the coexistence bulk density of the liquid and vapor phases, respectively. Technical details on how the density profile is determined accurately at different thermodynamic conditions are provided in the Supplementary Information section.

Once the equilibrium density profile ρ_{eq} is known, the surface tension may be determined from the simple thermodynamic identity

$$\gamma = \frac{\Omega + PV}{\mathscr{A}} \quad (8)$$

where $\mathscr{A}$ is the interfacial area and P is the bulk pressure.

3 Results

3.1 Vapor-liquid interfacial properties of Mie chain fluids

In this section we asses and discuss the accuracy of the new version of the density functional theory, based on the Helmholtz free energy of the SAFT-VR Mie approach, for describing interfacial behavior of chain molecules formed from Mie segments. In particular, we analyze the interfacial properties of chains formed from three, four, five, and six Mie segments with $\lambda_r = 10$ and $\lambda_a = 6$. Garrido *et al.*[83] have studied the interfacial properties of a number of Mie chain fluids combining MD simulations and the direct coexistence technique in inhomogeneous simulation boxes. In particular, they have used canonical simulations with fixed number of molecules N, fixed temperature T and an elongated simulation cell of constant volume. In this section, the attractive interaction parameter ε is chosen as the unit if energy and the Mie diameter as the unit of length. According to this, we define the following reduced quantities: temperature, $T^* = k_BT/\varepsilon$; density, $\rho^* = \rho\sigma^3$; surface tension, $\gamma^* = \gamma\sigma^2/\varepsilon$; and distance from the interface, $z^* = z/\sigma$.

The equilibrium density profiles $\rho(z)$ obtained by Garrido *et al.*[83], calculated in the usual way, are given in terms of the monomeric unit. Fig. 1a shows the segment density profiles $\rho(z)$ for Mie chains formed from two ($m_s = 2$) monomers (Mie dimers) at three different temperatures in the vapor-liquid coexistence region. We present the comparison between the results corresponding to the MD computer simulations performed by Garrido *at al.*[83] and theoretical predictions as obtained from the SAFT-VR Mie MF DFT approach developed in this work. For the shake of clarity, we only present one half of the profiles corresponding to one of the interfaces. Also for convenience, all density profiles have been shifted along z so as to place z_0, the Gibbs-diving surface, at the origin. The theory is able to predict the basic behavior of the density profiles as the temperature is increased and approaches to the critical temperature of the system: liquid density decreases, vapor density increases, and the absolute value of the slope of the density profiles in the interfacial region decreases as the temperature is increased. Agreement between simulation results and theoretical predictions is excellent at all temperatures, including the smooth variation of the density profiles along the interfacial region. Small differences are seen between simulation data and DFT predictions for the bulk liquid density at the highest temperature considered.

We also consider the density profiles of Mie chains formed from three ($m_s = 3$), four ($m_s = 4$) and five ($m_s = 5$) monomers at simi-

View Article Online
DOI: 10.1039/C9CP01597C

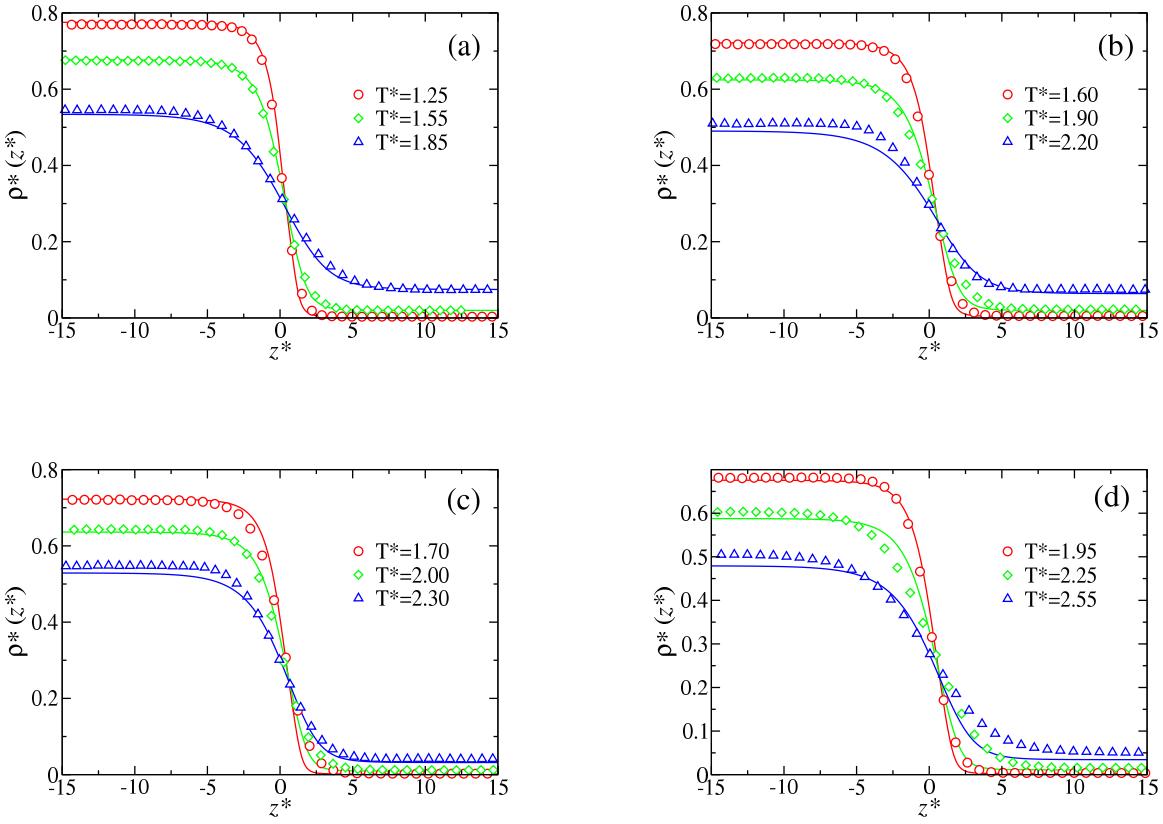

Fig. 1 Vapor-liquid density profiles $\rho(z)$ as functions of the distance from the interface z for Mie chains interacting by a Mie (10-6) potential and formed from two ($m_s = 2$) (a), three ($m_s = 3$) (b), four ($m_s = 4$) (c), and five ($m_s = 5$) monomeric segments (d) at several temperatures. The results obtained from the direct MD simulations of the inhomogeneous systems[83] orrespond to the symbols and the predictions from the proposed SAFT-VR Mie MF DFT are the curves.

View Article Online
DOI: 10.1039/C9CP01597C

lar conditions along the vapor-liquid coexistence region (Figs. 1b, 1c, and 1d, respectively). Agreement between theoretical predictions and simulation results of Garrido *et al.*[78] is also very good in all cases. In general, the behavior of the density profile in the interfacial region is well described. However, as the chain length is increased, differences between theory and simulation results increases. This is particularly clear in the case of chain formed from five Mie segments ($m_s = 5$). As can be seen, the slope of the density profiles at $T^* = 2.25$ and 2.55 deviates from simulation data. Simulation data suggest that the surface tension should be smaller than the value obtained from SAFT-VR Mie MF DFT, i.e., the absolute value of the slope of the density profile in the interfacial region obtained from theory is larger than that predicted from simulation data.

However, it is important to mention that results obtained from the theory are pure predictions from the information provided by the SAFT-VR Mie EOS: vapor and liquid coexistence densities and chemical potential at each temperature. In fact, the bulk values obtained from the limiting coexistence densities, calculated using the DFT far away from the interfacial region, are identical to those obtained using the bulk SAFT-VR EOS.

Once we have used the inhomogeneous theory to predict the structural behavior of Mie chains, we display the interfacial tension as a function of temperature for molecular chain fluids, $m_s = 1-6$, interacting through a Mie $(\lambda_r, 6)$ potential with $\lambda_r = 8$, 10, 12, and 20. We first consider a fixed Mie range $(8,6)$ and several values of the chain length m_s. Fig. 2a shows the interfacial tension as a function of temperature for this particular combination of the repulsive and attractive range values. The interfacial tension decreases as the temperature increases, showing the characteristic scaling law expected for this magnitude as the temperature approaches to the critical temperature[84]. As it occurs for the case of the density profiles, MD simulation results from Garrido *et al.*[83] and theoretical predictions from the DFT approach proposed in this work are in excellent agreement over a wide range of temperatures and chain lengths, including a satisfactory prediction of the region near the critical point. Unfortunately, theoretical predictions slightly overestimate the molecular simulation results as the chain length increases.

We have also determined the interfacial tension of Mie molecular chain fluids with the same chain lengths that interact through different Mie $(\lambda_r, 6)$ potentials. Figs. 2a, 2b, and 2c show the surface tension for systems interacting through $\lambda_r = 10$, 12, and 20. Agreement between both results (MD simulation and DFT) is also excellent in all cases.

It is very surprising how the combination of the SAFT-VR Mie EOS and the simplest DFT approach is able to predict accurately a key property such as surface tension, an interfacial property that is very sensitive to molecular details. It is important to remark here again that the version of DFT used in this work is a perturbative approach in which the reference contribution accounts for all the short-range molecular interactions in the system under the local density approximation. In addition to that, the perturbative term takes into account the long-range attractive dispersive interactions at the mean-field level of approximation, which is equivalent to neglect the correlations due to the attractive interactions.

The results presented in this work show the strength of a solid molecular-based theory, such as DFT, that is combined with an extremely precise and accurate EOS (SAFT-VR Mie). One of the key points of the successful prediction of surface tension values of molecular chains is the accuracy of the EOS predicting the vapor-liquid coexistence density at different temperatures, as it has been previously noticed by several authors[40,41,43].

However, it is also important to remark here that there exist differences between theoretical predictions and simulation results when the chain length is increased. The roots of these differences are due mainly to two reasons: (1) The MF version of the theory neglects the correlations due to the attractive interactions, producing differences between theory and simulation in the surface tension and structure of the density profiles, especially for long-chain molecules; (2) the SAFT approach is based on the linear approximation used to represent many-body correlations (in terms of pair distribution functions) within the Wertheim's theory treatment of the chain contribution (at the level of first-order approximation), providing a less accurate description of the vapor and liquid densities of chain molecules as chain length is increased.

3.2 Vapor-liquid interfacial properties of coarse-grained models

In last years, Jackson and collaborators have developed a series of force fields for different substances named generically SAFT-γ CG force fields[17–21]. These models are built using a coarse-graining strategy based on the idea that a wide range of real substances can be modeled effectively as chain molecules formed from chemical monomeric units that interact through the Mie potential. We take advantage of the work developed by these authors and use some of the CG models developed by them to predict the vapor-liquid interfacial properties of complex substances using the Helmholtz free energy functional presented in the previous section for Mie chain molecules. In particular, we concentrate here in two SAFT-γ CG force fields for the simulation of two important molecular fluids: the single-site CG model of carbon dioxide developed by Avendaño *et al.*[17] in 2011, and the more recent single-site CG model of water presented by Lobanova *et al.*[20] four years ago.

3.2.1 Single-site coarse-grained model of carbon dioxide

Carbon dioxide has recently become very important from scientific, economic, and environmental points of view as the urgent need to reduce its atmospheric presence. It is a small and rigid molecule and, a priori, seems to be very easy to model it. However, the presence of significant electrostatic interactions due to the electronegativity of the two oxygen atoms, makes the accurate molecular description a non-trivial problem.

Avendaño *et al.*[17] used the single-site SAFT-γ CG model of CO_2 to represent the thermodynamic properties of CO_2 with a state independent single-site spherical intermolecular potential. The model parameter values are estimated by optimizing the EOS for the vapor pressure and saturated liquid density over a range of subcritical temperatures. The authors used the grand canonical (GCMC) and isothermal-isobaric (NPT) ensembles, as well as the transition matrix Monte Carlo method in combination with the

View Article Online
DOI: 10.1039/C9CP01597C

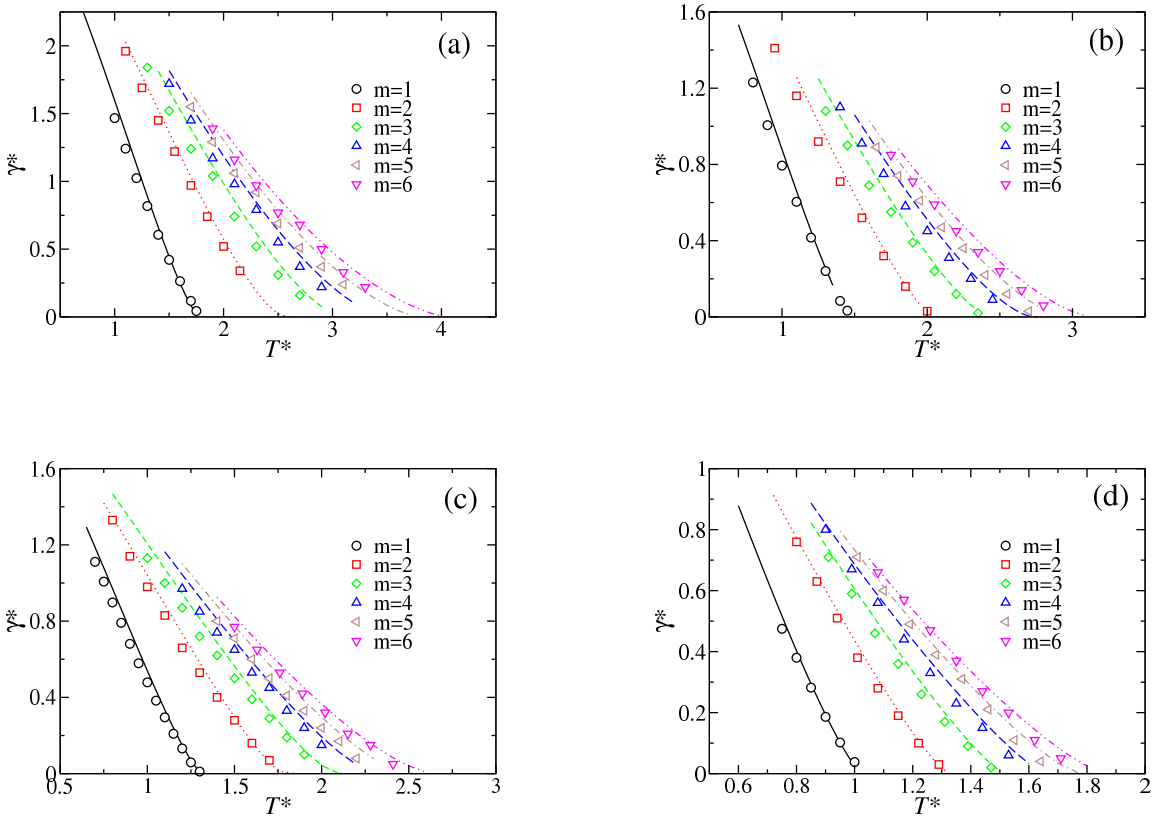

Fig. 2 Vapor-liquid surface tensions γ^* as functions of the temperature T^* for Mie chains interacting by a Mie (8-6) potential (a), (10-6) potential (b), (12-6) potential (c), and (20-6) potential (d) and formed from one (black circles), two (red squares), three (green diamonds), four (blue up triangles), five (brown left triangles), and six (magenta down triangles) monomeric segments. The symbols correspond to the results obtained from the direct MD simulations of the inhomogeneous systems[83] and the curves are the redictions from the proposed SAFT-VR Mie MF DFT.

View Article Online
DOI: 10.1039/C9CP01597C

histogram reweighting technique to determine different thermodynamic properties, including enthalpy of vaporization, supercritical densities, second-derivative properties, and surface tension. Unfortunately, they do not present results for the density profiles associated to the vapor-liquid interface since they do not simulate the interface explicitly.

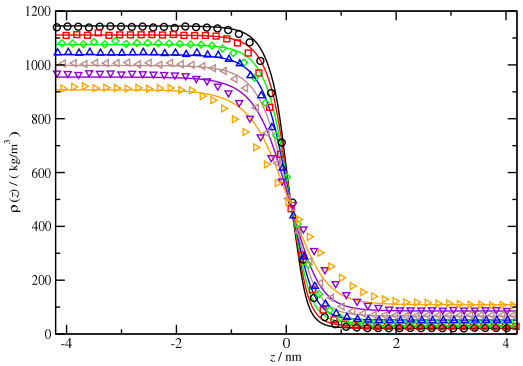

Fig. 3 Vapor-liquid density profiles $\rho(z)$ as functions of the distance from the interface z for CO_2. The curves correspond to the predictions obtained from the SAFT-VR Mie MF DFT formalism and symbols correspond to the MD-NVT simulations obtained in this work at different temperatures: 226.06 K (black curve and circles), 235.10 K (red curve and squares), 244, 145 K (green curve and diamonds), 253.18 K (blue curve and up triangles), 262.23 K (brown curve and left triangles), 271.27 K (violet curve and down triangles), and 280.31 K (orange curve and right triangles).

Since we are interesting in the interfacial behavior of this model in order to investigate the ability of the SAFT-VR Mie MF DFT approach presented in this work, we have performed additional computer simulations to determine some vapor-liquid interfacial properties of the model. In particular, we use the direct coexistence technique in the NVT canonical ensemble. All MD simulations are performed using GROMACS (version 4.6.1). Computer simulation details are similar to those presented in a recent paper[85]. Following the approach described by Garrido *et al.*[78], we have determined the equilibrium density profiles $\rho(z)$ of CO_2 from MD-NVT simulations. Additionally, we have also obtained the density profiles from the SAFT-VR Mie MF DFT formalism. Fig. 3 shows the density profiles $\rho(z)$ for CO_2 at different temperatures in the vapor-liquid coexistence region. We present the comparison between the results obtained from MD-NVT computer simulations performed in this work and the theoretical predictions as obtained from the SAFT-VR Mie MF DFT approach. As in the case for Mie chains, we only present one half of the profiles corresponding to one of the interfaces and all the density profiles have been shifted along z so as to place the Gibbs-diving surface at the origin.

The theory and simulation results show the characteristic behavior of the density profiles as the temperature is varied, from the lowest temperature (226 K) up to the highest temperature (298 K) considered. The SAFT-VR Mie MF DFT is able to predict accurately the bulk values of the vapor and liquid densities. This is an expected result since the functional theory reduces to the SAFT-VR Mie EOS in the bulk limit. However, small differences between theoretical predictions and computer simulation results are seen at the interfacial region. In particular, density profiles predicted by the SAFT-VR Mie MF DFT formalism slightly overestimates the density in the liquid-like part of the profile and underestimates the density in the vapor-like region of the interface. Differences between theory and simulations seem to increase as the temperature of the system is increased. This is an expected result since the system approaches to the critical point as the temperature increases. It is important to take into account that the formalism presented here does not incorporate the correct density fluctuations that occur in the system when the temperature approaches to the critical point.

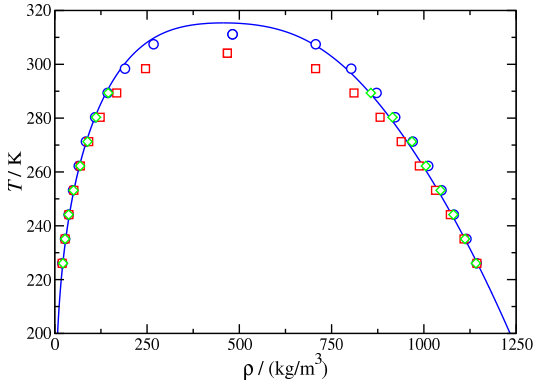

Fig. 4 Vapor-liquid coexistence densities of CO_2. The red squares correspond to smooth experimental coexistence densities taken from NIST[86], the blue circles the coexistence densities obtained by Avendaño *et al.*[17] using GC-MC simulations, the green diamonds the coexistence densities using the MD-NVT simulations obtained in this work, and curve denotes the predictions from the SAFT-VR Mie MF DFT formalism in the bulk limit (SAFT-VR Mie EOS) for the SAFT-γ CG Mie model of CO_2.

From the analysis of the density profiles obtained from the MD-NVT simulations it is possible to calculate the vapor-liquid phase envelope of the system in a wide range of temperatures. Fig. 4 shows the temperature density or $T-\rho$ projection of the phase diagram of CO_2 as obtained from theory and simulation. We have also included experimental data taken from NIST[86], as well as the simulation results obtained from Avendaño *et al.*[17] In addition to that, we also show the predictions from the SAFT-VR Mie EOS, which corresponds to the results of the DFT in the bulk limit. As can be seen, the simulation results obtained in this work are in good agreement with simulations for the SAFT-γ CG model of Avendaño *et al.*[17], the theory, and the experimental vapor-liquid coexistence envelope. Close to the critical point, however, agreement between experiments and simulation and theory is not so good. This is expected since the theory does not take into account for fluctuations of the system close to the critical point. Additionally, GC-MC and MD-NVT direct coexistence techniques also overestimate the critical temperature since a full finite-size

View Article Online
DOI: 10.1039/C9CP01597C

scaling treatment is not used.

We have used the SAFT-VR Mie MD Mie DFT formalism developed in this work to predict the vapor-liquid surface tension of the CG CO_2 model developed by Avendaño *et al.* We have also determined the interfacial tension of the model using MD-NVT simulations from the diagonal components of pressure tensor and its mechanical definition. Fig. 5 shows the surface tension as as function of the temperature for CO_2. Simulation results obtained in this work follow the same trend as those presented by Avendaño *et al.*[17] although it underestimate the surface tension values in nearly the whole range of temperatures considered. This is probably due to the different methodologies employed in both sets of simulations. In our case, we use the direct simulation technique to simulate to interface of CO_2. As a consequence of this, we use a cutoff distance $r_c = 6\sigma$, with $\sigma = 0,.374\,\text{nm}$ the size of the spherical site of CO_2. However, Avendaño *et al.*[17] have obtained the surface tension of the system using the well-known finite-size scaling formalism of Binder[87], in combination with bulk GC-MC simulations using a cutoff distance $r_c = 4\sigma$ and standard long-range corrections to the energy and pressure virial. This methodology allows to determine the surface tension in the thermodynamic limit from the extrapolation of a series of simulations for systems of different sizes. The advantage of this technique is that also provides an accurate estimate of the critical point of the system.

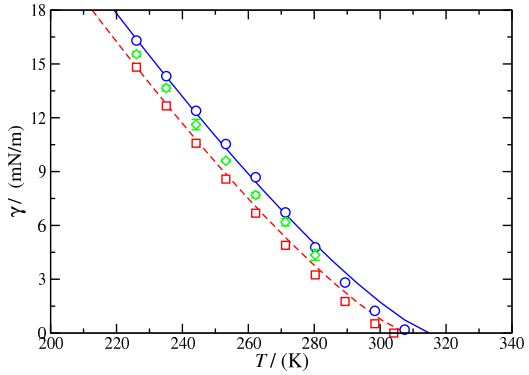

Fig. 5 Vapor-liquid surface tension of CO_2. The red squares correspond to smooth experimental data taken from NIST[86], the blue circles the surface tension values obtained by Avendaño *et al.* using GC-MC simulations, the green diamonds the surface tension values using the MD-NVT simulations obtained in this work, the continuous blue curve denotes the predictions from the SAFT-VR Mie MF DFT formalism for the SAFT-γ CG Mie model of CO_2 with the original optimization of Avendaño *et al.*[17], and the dashed red curve the predictions from the SAFT-VR Mie MF DFT for the SAFT-γ CG Mie model of CO_2 rescaled to match the critical temperature.

We have compared the theoretical predictions as obtained from the DFT formalism with experimental data taken from the literature. As can be seen, the three predictive methodologies, theory, GC-MD, and MD-NVT computer simulations, lead to a reasonable description of the experimental surface tension values with a small overestimate of the interfacial tension. Avendaño *et al.* explained the discrepancies in terms of the overprediction of the critical point of the model that shifts the surface tension curve of the model an almost constant amount over the entire range of coexistence temperatures.

Finally, it is important to mention that the SAFT-γ CG Mie model can be refined to describe accurately the interfacial tension of CO_2, as well as the saturation curve, ensuring that the model reproduces the experimental critical temperature (see Fig. 4 of the work of Avendaño *et al.*[17]). Following the same approach, we have rescaled the potential energy parameter from $\varepsilon/k_B = 361.69\,\text{K}$ to $\varepsilon/k_B = 353.55\,\text{K}$ in the SAFT-VR Mie MF DFT formalism. The interfacial tension obtained from the theory using the rescaled model is also shown in Fig. 5. In this case, as it happens with computer simulation results of Avendaño *et al.*[17] (see Fig. 4 of their work), agreement between theoretical predictions and experimental is excellent in the whole range of temperatures.

3.2.2 Single-site coarse-grained model of water

Water is the most abundant liquid on earth and perhaps the most important liquid in nature, being a common solvent in industrial and biological systems. In spite of its apparent simplicity as a liquid, accurate modeling of its structural and/or thermodynamic properties as pure component or in aqueous solution mixtures still remains one of the most challenging research in chemical physical and physical chemistry. Similarly to the work of Avendaño *et al.*[17], Lobanova *et al.*[20] have proposed a single-site CG model of water applicable over a wide range temperature range. They model interactions between water molecules with a single CG spherical site interacting via the Mie intermolecular potential to capture the effective interactions between them. One of the models proposed in their original work, the Mie (8-6) CG model of water (CGW1-ift), is especially designed to target saturated-liquid density and vapor-liquid interfacial tension. The size $\sigma(T)$ and energy $\varepsilon(T)$ parameters are estimated directly from molecular simulation data for saturated-liquid density and vapor-liquid interfacial tension at each temperature (see Table 4 of Lobanova *et al.*[20] for further details).

The authors determined the thermodynamic behavior of water from MD simulations using the direct coexistence technique in the NVT canonical ensemble. In particular, they obtained different thermodynamic properties, including vapor-liquid coexistence densities, saturated vapor pressure, entalphy of vaporization, and interfacial tension. In this later case, the authors used both the mechanical and thermodynamic (Test-Area method of Gloor *et al.*[88]) routes to determined the surface tension. It is important to recall here that the parametrization of the model proposed by Lobanova *et al.*[20] uses a cutoff distance $r_c = 20\,\text{Å}$, which corresponds to a reduced cutoff distance varying from $r_c^* \approx 6.88$ at low temperature (293 K) up to $r_c^* \approx 6.98$ at high temperature (493 K), approximately.

As in the case of the CG CO_2 model, we have performed MD simulations using the direct coexistence technique in the NVT canonical ensemble to determine the equilibrium density profiles of H_2O. Fig. 6 shows the density profiles $\rho(z)$ of H_2O at different temperatures in the vapor-liquid coexistence region. The density

View Article Online
DOI: 10.1039/C9CP01597C

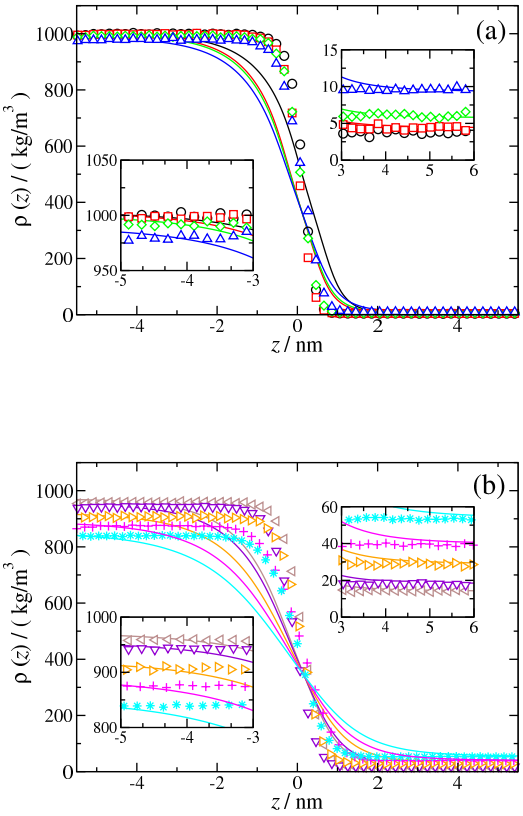

Fig. 6 Vapor-liquid density profiles $\rho(z)$ as functions of the distance from the interface z for H_2O. The curves correspond to the predictions obtained from the SAFT-VR Mie MF DFT formalism and symbols correspond to the MD-NVT simulations obtained in this work at different temperatures: (a) 293 K (black curve and circles), 298.10 K (red curve and squares), 313, 145 K (green curve and diamonds), 343.18 K (blue curve and up triangles); (b) 373.23 K (brown curve and left triangles), 393.27 K (violet curve and down triangles), 433.31 K (orange curve and right triangles), 463.31 K (magenta curve and pluses), and 493.31 K (cyan curve and stars). The left and right insets show to the liquid-like and vapor-like regions of the density profiles, respectively.

profiles exhibit the qualitative behavior expected. Agreement between theoretical predictions and MD-NVT computer simulations for the bulk values of the vapor and liquid densities is excellent in all cases. Insets of Fig. 6 show the comparison between theory and simulation for the liquid phase (left inset) and the vapor phase (right inset). Unfortunately, the theory is unable to predict quantitatively the variation of the density along the interface from the vapor to the liquid phase. In particular, theoretical predictions overestimates the density of the vapor-like region of the density profiles and underestimates the density in the liquid-like region. Differences between theory and computer simulation increase as the temperature is increased. SAFT-VR Mie MF DFT predicts wider interfacial regions between the liquid- and vapor-like zones at each temperature considered. In fact, density profiles obtained from MD-NVT computer simulations are sharper than those predicted by the theory, which results in low interfacial thickness values. Differences between theory and simulation in the region at which density varies continuously from vapor to liquid have also seen previously in the case of the CG CO_2. We think these differences are mainly due to the approximations made in the construction of the density functional. In the mean-field version of the theory presented in this work, correlations between pair molecules due to the attractive interactions are neglected. This behavior have been previously seen in density functional based on SAFT-like Helmholtz free energies.[40–44,77]

We have obtained the vapor-liquid phase coexistence diagram of the CG H_2O model from the information of the $\rho(z)$ density profiles calculated from the MD-NVT simulations. In addition to that, we have also determined the coexistence curve using the SAFT-VR Mie EOS and compared the theoretical predictions with computer simulation results and experimental data taken from the literature.[86] As can be seen in Fig. 7, the theory and simulation results are in excellent agreement in a wide range of temperatures. For comparison reasons, we have also included the MC-NVT simulation data obtained by Lobanova *et al.*[20] Note that simulation results obtained independently from MC and MD are in excellent agreement in all cases. The saturated-liquid densities obtained by simulation and theory are in excellent agreement with the experimental data over the entire fluid temperature range. However, saturated-vapor densities are slightly overestimated, especially at high temperatures. This result is expected since only saturated-liquid densities where employed in the parametrization. As discussed by Lobanova *et al.*[20], CG models of the type used for H_2O, in which the size $\sigma(T)$ and energy $\varepsilon(T)$ parameters must be temperature dependent in order to predict accurately the behavior of a given number of properties. This is especially critical when modeling highly anisotropic and short-ranged molecular interactions using simplified single-site spherical isotropic models that do not take into account explicitly these microscopic characteristics.

Finally, we have used the SAFT-VR Mie MF DFT formalism to determine the vapor-liquid surface tension of the model. The interfacial tension has also been calculated from the diagonal components of the pressure tensor using MD-NVT simulations. Fig. 8 shows the surface tension as a function of the temperature in the entire fluid range of water. We have also included the simula-

View Article Online
DOI: 10.1039/C9CP01597C

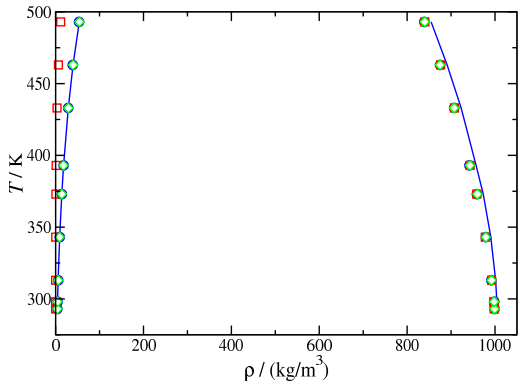

Fig. 7 Vapor-liquid coexistence densities of H_2O. The red squares correspond to smooth experimental coexistence densities taken from NIST[86], the blue circles the coexistence densities obtained by Lobanova *et al.*[20] using MD-NVT simulations, the green diamonds the coexistence densities using the MD-NVT simulations obtained in this work, and curve denotes the predictions from the SAFT-VR Mie MF DFT formalism in the bulk limit (SAFT-VR Mie EOS) for the SAFT-γ CG Mie model of H_2O.

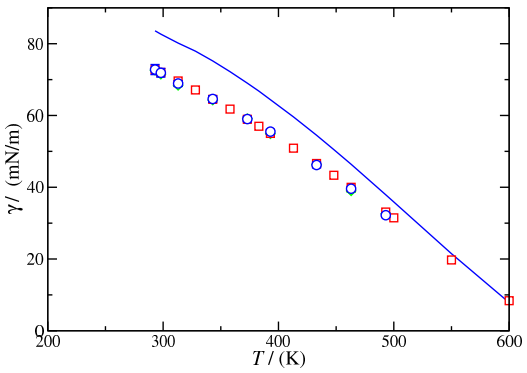

Fig. 8 Vapor-liquid surface tension of H_2O. The red squares correspond to smooth experimental data taken from NIST[86], the blue circles the surface tension values obtained by Lobanova *et al.*[20] using MD-NVT simulations, the green diamonds the surface tension values using the MD-NVT simulations obtained in this work, and the continuous blue curve denotes the predictions from the SAFT-VR Mie MF DFT formalism for the SAFT-γ CG Mie model of H_2O.

tion results obtained from Lobanova *et al.*[20] using MC-NVT simulations, as well as the experimental data taken from the literature[86]. MD and MC computer simulation values corresponding to the CG H_2O model are in excellent agreement with experimental data in the whole range of temperatures considered. Theoretical predictions from the SAFT-VR Mie MF DFT describe qualitatively the behavior of the vapor-liquid surface tension. As can be seen, the theory overestimates the simulation and experimental data at low temperatures, although it provides an accurate description of the vapor-liquid interfacial tension at high temperatures. It is important to mention that the theory is also able to predict the correct sigmoidal shape of the surface tension curve, as a function of the temperature, exhibited by associating systems such as water. The SAFT-VR Mie MF DFT approach provides a better description of the surface tension for temperatures approaching to critical point. A similar result was obtained using the mean-field approximation in the context of the SAFT-VR DFT version based on the SAFT-VR Helmholtz free energy for molecules interacting through the SW intermolecular potential proposed by Gloor *et al.*[43] It is expected that the incorporation of correlations in the perturbative term greatly improves the theoretical description of the surface tension at lower temperatures. This will be the subject of a future work.

4 Conclusion

We have extended the general SAFT-VR DFT formalism proposed by Gloor *et al.*[43] originally developed to predict the interfacial properties of pure fluids that interact through the square-well intermolecular potential to deal with chain molecules formed from monomeric units that interact via the Mie intermolecular potential. The new DFT formalism is based on the last version of the statistical associating fluid theory for potentials of variable range for homogeneous Mie chainlike fluids (SAFT-VR Mie EOS) according to the following approximations: (1) the reference term contains all the short-range interactions treated at the local level; (2) the perturbative contribution accounts for the attractive long-range dispersive interactions; and (3) the attractive term is described using a mean-field approach in which pair correlations due to attractions are neglected.

The new approach has been used to examine the influence of the molecular chain length and the repulsive exponent of the intermolecular potential on the interfacial phenomena for chain models made up to six Mie $(\lambda_r - 6)$ segments with different values of the repulsive exponent of the intermolecular potential. In particular, the density profiles and interfacial tension are seen to be very sensitive to the chain length and dispersive energies. This analysis provides a molecular based understanding of the microscopic features that control the interfacial properties of chainlike molecules. Agreement between theoretical predictions and computer simulations of the same models taken from literature and from simulation results obtained in this work is excellent in all systems considered and at all thermodynamic conditions considered.

Once the formalism have demonstrated that is able to predict with confidence the interfacial properties of chain molecules that interact via the Mie intermolecular potential, the SAFT-VR Mie MF DFT approach has been used to predict the vapor-liquid interfacial properties of real molecules. In particular, in this preliminary work we examine the interfacial properties of two coarse-graining models proposed recently to describe the phase equilibria of carbon dioxide[17] and water[20]. Agreement between the theoretical predictions, computer simulation results performed by the original authors of the models and by us, and existing experimental data for the vapor-liquid interfacial tension is very good, particularly in the case of carbon dioxide. The theoretical framework developed in this work opens up a wide variety of possibilities,

View Article Online
DOI: 10.1039/C9CP01597C

enabling a determination of the interfacial properties of complex substances in a confidence and fully predictive manner.

Currently, we are working on the application of the theory to predict the interfacial properties of real chain molecules. We expect a good description of the interfacial tension, and particularly density profiles and surface tension, mainly due to two reasons: (1) Agreement between density profiles and vapour-liquid interfacial tension obtained from molecular simulation and DFT is excellent; therefore, we expect a similar agreement with systems for which the number of segments is less or similar; (2) a DFT model usually provides a good description of surface tension if the theory, in the bulk limit, is able to predict accurately the vapor and liquid coexistence densities. In the particular case of the theoretical framework presented in this paper, the bulk limit of the DFT corresponds to the SAFT-VR Mie EOS, one of the most accurate and versatile SAFT version in the literature.

5 Acknowledgement

The authors thank helpful discussions with Carlos Avendaño and José Matías Garrido. We also acknowledge Centro de Supercomputación de Galicia (CESGA, Santiago de Compostela, Spain) and MCIA (Mésocentre de Calcul Intensif Aquitain) of the Universités de Bordeaux and Pau et Pays de l'Adour (France), for providing access to computing facilities and Ministerio de Economía, Industria y Competitividad through Grant with reference FIS2017-89361-C3-1-P co-financed by EU FEDER funds. Further financial support from Junta de Andalucía and Universidad de Huelva is also acknowledged. J.A., J.M.M., and F.J.B. thankfully acknowledge the computer resources at Magerit and the technical support provided by the Spanish Supercomputing Network (RES) (Project QCM-2018-2-0042).

References

1 W. G. Chapman, K. E. Gubbins, G. Jackson and M. Radosz, *Fluid Phase Equil.*, 1989, **52**, 31–38.
2 W. G. Chapman, K. E. Gubbins, G. Jackson and M. Radosz, *Ind. Eng. Chem. Res.*, 1990, **29**, 1709–1721.
3 M. S. Wertheim, *J. Stat. Phys.*, 1984, **35(1-2)**, 19–34.
4 M. S. Wertheim, *J. Stat. Phys.*, 1984, **35(1-2)**, 35–47.
5 M. S. Wertheim, *J. Stat. Phys.*, 1986, **42(3-4)**, 459–476.
6 M. S. Wertheim, *J. Stat. Phys.*, 1986, **42**, 477–492.
7 A. Gil-Villegas, A. Galindo, P. J. Whitehead, S. J. Mills, G. Jackson and A. N. Burgess, *J. Chem. Phys.*, 1997, **106**, 4168–4186.
8 A. Galindo, L. A. Davies, A. Gil-Villegas and G. Jackson, *Mol. Phys.*, 1998, **93**, 241–252.
9 F. J. Blas and L. F. Vega, *Mol. Phys.*, 1997, **92**, 135.
10 F. J. Blas and L. F. Vega, *Ind. Eng. Chem. Res.*, 1998, **37**, 660.
11 J. Gross and G. Sadowski, *Ind. Eng. Chem. Res.*, 2002, **41**, 1084–1093.
12 Georgios M. Kontogeorgis, Epaminondas C. Voutsas, Iakovos V. Yakoumis, and Dimitrios P. Tassios, *Ind. Eng. Chem. Res.*, 1996, **35**, 4310–4318.
13 M. M. P. T. Lafitte and J. L. Daridon, *J. Chem. Phys.*, 2006, **124**, 024509/1–16.
14 T. Lafitte, A. Apostolakou, C. Avendaño, A. Galindo, C. S. Adjiman, E. A. Müller and G. Jackson, *J. Chem. Phys.*, 2013, **139**, 154504.
15 E. A. Müller and G. Jackson, *Annu. Rev. Chem. Biomol. Eng.*, 2014, **5**, 405–427.
16 C. Herdes, T. S. totton and E. A. Müller, *Fluid Phase Equilib.*, 2015, **406**, 91–100.
17 C. Avendaño, T. Lafitte, A. Galindo, C. S. Adjiman, G. Jackson and E. A. Müller, *J. Phys. Chem. B*, 2011, **115**, 11154–11169.
18 C. Avendaño, T. Lafitte, C. S. Adjiman, A. Galindo, E. A. Müller and G. Jackson, *J. Phys. Chem. B*, 2013, **117(9)**, 2717–2733.
19 T. Lafitte, C. Avendaño, V. Papaionnou, A. Galindo, C. S. Adjiman, G. Jackson and E. A. Müller, *Mol. Phys.*, 2012, **110(11-12)**, 1189–1203.
20 O. Lobanova, T. Lafitte, C. Avendaño, E. A. Müller and G. Jackson, *Mol. Phys.*, 2015, **113**, 1228–1249.
21 G. J. O. Lobanova, A. Mejía and E. A. Müller, *J. Chem. Thermodynamics*, 2016, **93**, 320–336.
22 J. D. V. D. Waals, *Z. Phys. Chem.*, 1894, **13**, 657.
23 J. W. Cahn and J. E. Hilliard, *J. Chem. Phys.*, 1958, **28**, 258–267.
24 B. S. Carey, H. T. Davis and L. E. Scriven, *AIChE J.*, 1978, **24**, 1076–1080.
25 B. S. Carey, H. T. Davis and L. E. Scriven, *AIChE J.*, 1980, **26(5)**, 705–711.
26 B. S. Carey, *PhD thesis*, University of Minnesota, 1979.
27 H. T. Davis, *Statistical Mechanics of Phases, Interfaces, and Thin Films*, VCH, Weinheim, 1996.
28 R. Evans, *Density Functionals in the Theory of Nonuniform Fluids. In Fundamentals of Inhomogeneous Fluids*, Dekker, New York, 1992.
29 H. Löwen, *J. Phys.: Condens. Matter*, 2002, **14**, 11987–11905.
30 J. Wu, *AIChE Journal.*, 2006, **52**, 1169–1193.
31 J. Wu and Z. Li, *Annu. Rev. Phys. Chem.*, 2007, **58**, 85–112.
32 Y. Rosenfeld, *Phys. Rev. Lett.*, 1989, **63**, 980–983.
33 R. Roth, R. Evans, A. Lang and G. Kahl, *J. Phys.: Condens. Matter*, 2002, **14**, 12063–12078.
34 Y. X. Yu and J. Wu, *J. Chem. Phys.*, 2002, **116(16)**, 7094–7103.
35 Y. X. Yu and J. Z. Wu, *J. Chem. Phys.*, 2002, **117**, 2368–2376.
36 S. Tripathi and W. G. Chapman, *J. Chem. Phys.*, 2005, **122**, 094506/1–11.
37 S. Tripathi, A. Dominik and W. G. Chapman, *Ind. Eng. Chem. Res.*, 2006, **45**, 6785–6792.
38 S. Jain, A. Dominik and W. G. Chapman, *J. Chem. Phys.*, 2007, **127**, 244904/1–12.
39 P. Bryk, K. Bucior and S. Sokolowski, *J. Phys. Chem. C*, 2007, **111**, 15523–15532.
40 F. Llovell, A. Galindo, G. Jackson and F. J. Blas, *J. Chem. Phys.*, 2010, **133**, 024704/1–19.
41 F. J. Blas, E. Martín Del Río, E. de Miguel and G. Jackson, *Mol. Phys.*, 2001, **99**, 1851–1865.
42 G. J. Gloor, F. J. Blas, E. M. D. Río, E. D. Miguel and G. Jack-

View Article Online
DOI: 10.1039/C9CP01597C

son, *Fluid Phase Equil.*, 2002, **194-197**, 521–530.
43 G. J. Gloor, G. Jackson, F. J. Blas, E. Martín Del Río and E. D. Miguel, *J. Chem. Phys.*, 2004, **121**, 12740–12759.
44 G. J. Gloor, G. Jackson, F. J. Blas, E. M. D. Río and E. D. Miguel, *J. Phys. Chem. C*, 2007, **111**, 15513–15522.
45 J. Winkelmann, *Mol. Phys.*, 2001, **13**, 4739–4768.
46 H. Kahl, M. Mecke and J. Winkelmann, *Fluid Phase Equil.*, 2005, **228-229**, 293–302.
47 H. Kahl and J. Winkelmann, *Fluid Phase Equil.*, 2008, **270**, 50–61.
48 C. P. Emborsky, Z. Feng, K. R. Cox and W. G. Chapman, *Fluid Phase Equil.*, 2011, **306**, 15–30.
49 S. Tripathi and W. G. Chapman, *Phys. Rev. Lett.*, 2005, **94**, 087801/1–4.
50 A. Bymaster, S. Jain and W. G. Chapman, *J. Chem. Phys.*, 2008, **128**, 164910/1–13.
51 S. Jain and W. G. Chapman, *Mol. Phys.*, 2009, **107**, 1–17.
52 S. Jain, V. V. Ginzburg, P. Jog, J. Weinhold, R. Srivastava and W. G. Chapman, *J. Chem. Phys.*, 2009, **131**, 044908/1–14.
53 C. P. Emborsky, K. R. Cox and W. G. Chapman, *J. Chem. Phys.*, 2011, **135**, 084708/1–15.
54 L. Wang, A. Haghmoradi, J. Liu, S. Xi, G. J. Hirasaki, C. A. Miller and W. G. Chapman, *J. Chem. Phys.*, 2017, **146**, 124705/1–12.
55 K. Gong, B. D. Marshall and W. G. Chapman, *J. Chem. Phys.*, 2013, **139(9)**, 094904/1–8.
56 D. Ballal and W. G. Chapman, *J. Chem. Phys.*, 2013, **139**, 114706/1–11.
57 A. Dominik, S. Tripathi and W. G. Chapman, *Industrial & Engineering Chemistry Research*, 2006, **45(20)**, 6785–6792.
58 E. Kierlik and M. L. Rosinberg, *J. Chem. Phys.*, 1992, **97(12)**, 9222–9239.
59 E. Kierlik and M. L. Rosinberg, *J. Chem. Phys.*, 1993, **99(5)**, 3950–3965.
60 E. Kierlik and M. L. Rosinberg, *J. Chem. Phys.*, 1994, **100(2)**, 1716–1730.
61 D. Cao and J. Wu, *J. Chem. Phys.*, 2004, **121(9)**, 4210–4220.
62 M. Cao, A.P. Malanoski, J.W. Schroer and P.A. Monson, *Fluid Phase Equil.*, 2005, **228–229**, 72–82.
63 P. Bryk, K. Bucior, S. Sokołowski and G. Żukociński, *The Journal of Physical Chemistry B*, 2005, **109(7)**, 2977–2984.
64 P. Bryk, O. Pizio and S. Sokołowski, *The Journal of Chemical Physics*, 2005, **122(17)**, 174906–7.
65 P. Bryk, K. Bucior, S. Sokolowski and G. Zukocinski, *J. Phys.: Condens. Matter*, 2004, **16**, 8861–8873.
66 A. Malijevskỳ, P. Bryk and S. Sokołowski, *Physical Review E*, 2005, **72(3)**, 032801–4.
67 J. Gross, *J. Chem. Phys.*, 2009, **131**, 204705/1–12.
68 X. Tang and J. Gross, *J. Supercrit. Fluids*, 2010, **55**, 735–742.
69 C. Klink and J. Gross, *Ind. Eng. Chem. Res.*, 2014, **53(14)**, 6169–6178.
70 C. K. B. Planková and J. Gross, *Ind. Eng. Chem. Res.*, 2015, **54(16)**, 4633–4642.
71 E. Sauer and J. Gross, *Ind. Eng. Chem. Res.*, 2017, **56(14)**, 4119–4135.
72 G. Jackson, W. G. Chapman and K. E. Gubbins, *Mol. Phys.*, 1988, **65**, 1–31.
73 W. G. Chapman, G. Jackson and K. E. Gubbins, *Mol. Phys.*, 1988, **65**, 1057–1079.
74 G. Jackson, *Mol. Phys.*, 1991, **72**, 1365–1385.
75 S. toxvaerd, *J. Chem. Phys.*, 1976, **64(7)**, 2863–2867.
76 N. Mac Dowell, F. Pereira, F. Llovell, F. Blas, C. Adjiman, G. Jackson and A. Galindo, *The Journal of Physical Chemistry B*, 2011, **115**, 8155–8168.
77 F. Llovell, N. MacDowell, A. Galindo, G. Jackson and F. J. Blas, *Fluid Phase Equil.*, 2012, **336**, 137–150.
78 J. M. Garrido, J. Algaba, J. M. Míguez, B. Mendiboure, A. I. Moreno-Ventas Bravo, M. M. Piñeiro and F. J. Blas, *J. Chem. Phys.*, 2016, **144**, 144702/1–11.
79 G. Mie, *Ann. Phys. (Berlin)*, 1903, **316(8)**, 657–697.
80 E. Gruneisen, *Ann. Phys. (Berlin)*, 1912, **344**, 257–306.
81 J. E. Jones, *Proc. R. Soc. Lond. A*, 1924, **106**, 441–462.
82 J. Lennard-Jones, Proc. Phys. Soc.(London), 1931, p. 461.
83 J. M. Garrido, M. M. Piñeiro, A. Mejía and F. J. Blas, *Phys. Chem. Chem. Phys.*, 2016, **18**, 1114–1124.
84 F. J. Blas, F. J. Martínez-Ruiz, A. I. Moreno-Ventas Bravo and L. G. MacDowell, *J. Chem. Phys.*, 2012, **137**, 024702.
85 J. Algaba, J. M. Garrido, J. M. Míguez, A. Mejía, A. I. M.-V. Bravo and F. J. Blas, *J. Phys. Chem. C*, 2018, **122**, 16142–16153.
86 P. Linstrom and W. Mallard, *NIST Chemistry Webbook, NIST Standard Reference Database Number 69, Https://webbook.nist.gov, (retrieved September, 2015)*.
87 K. Binder, *Phys. Rev. A*, 1982, **25(3)**, 1699.
88 G. J. Gloor, G. Jackson, F. J. Blas and E. D. Miguel, *J. Chem. Phys.*, 2005, **123**, 134703/1–19.